1 Supplementary material for paper LHCb-PAPER-2014-018

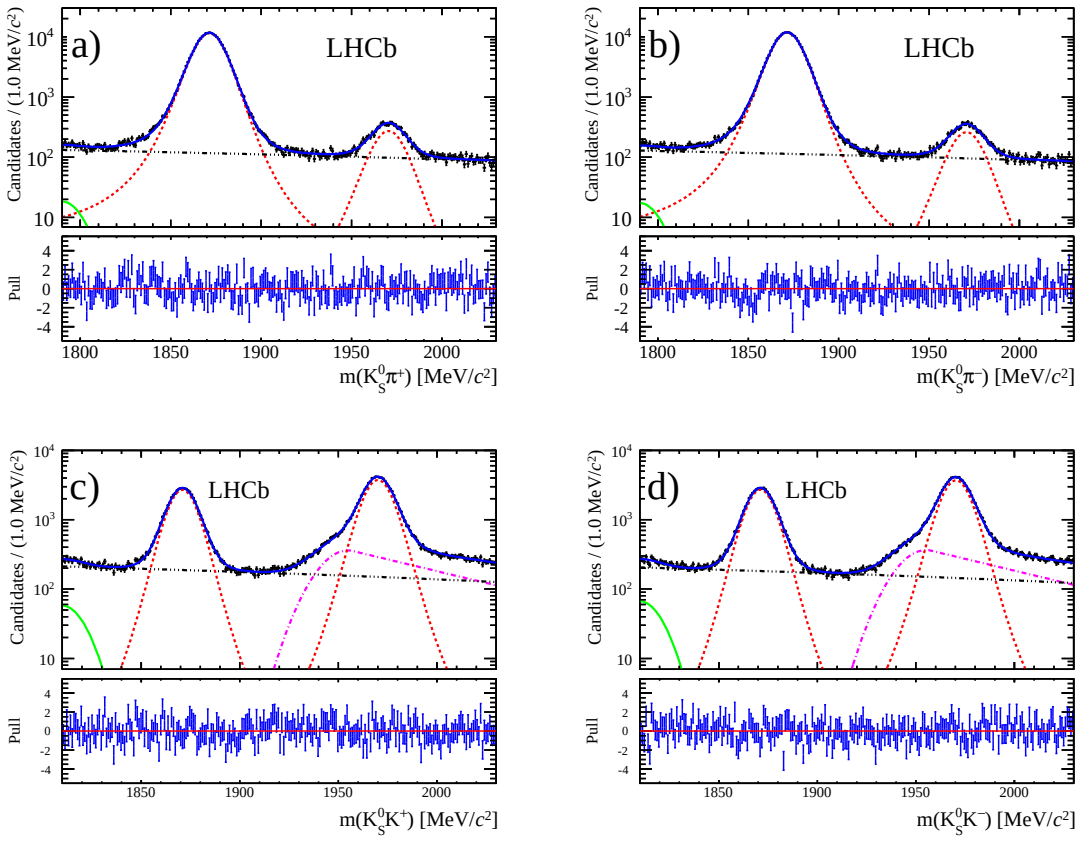

Figure 1: Invariant mass distributions for the a) $D^+_{(s)} \to K^0_S\pi^+$, b) $D^-_{(s)} \to K^0_S\pi^-$, c) $D^+_{(s)} \to K^0_S K^+$ and d) $D^-_{(s)} \to K^0_S K^-$ decay candidates for data taken in the magnetic polarity *Up* configuration at $\sqrt{s} = 7$ TeV. The data are shown as black points and the total fit function by a blue line. The contributions from the signal, and the low-mass, cross-feed and combinatorial backgrounds are indicated by red (dotted), green (full), magenta (dash-dotted) and black (multiple-dot-dashed) lines, respectively. The bottom figures are the normalised residuals (pull) distributions.

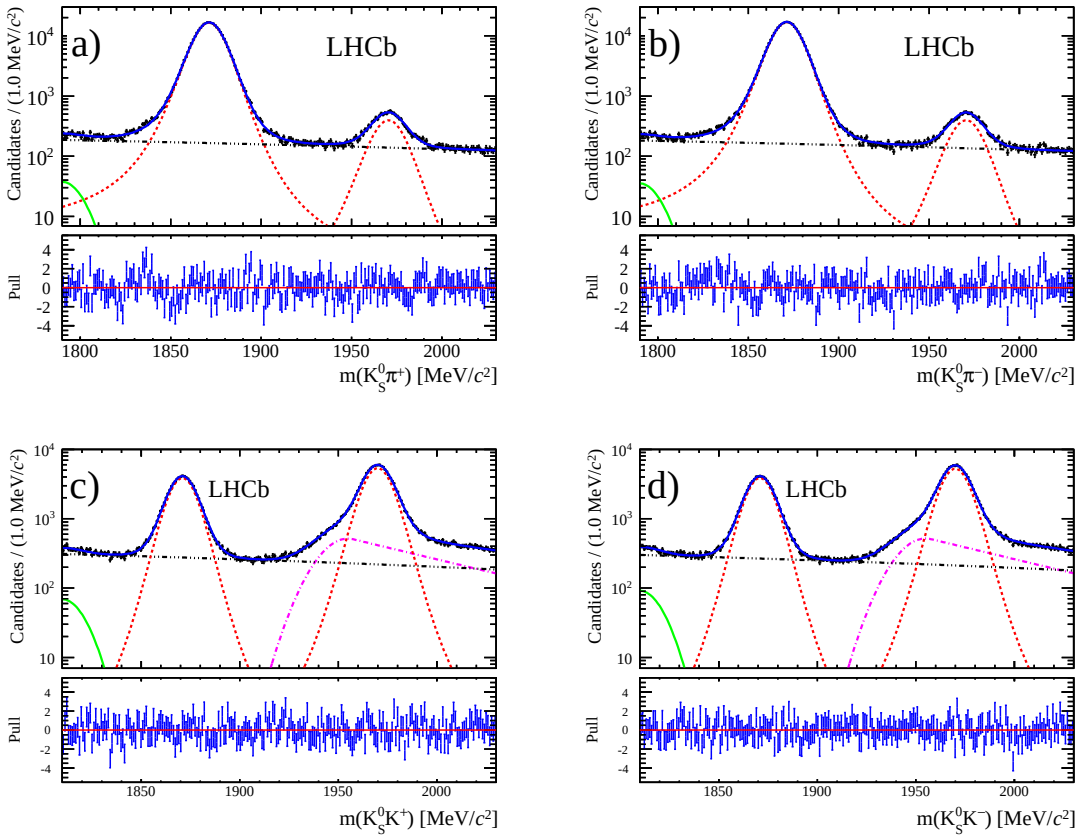

Figure 2: Invariant mass distributions for the a) $D^+_{(s)} \to K^0_S\pi^+$, b) $D^-_{(s)} \to K^0_S\pi^-$, c) $D^+_{(s)} \to K^0_S K^+$ and d) $D^-_{(s)} \to K^0_S K^-$ decay candidates for data taken in the magnetic polarity *Down* configuration at $\sqrt{s} = 7$ TeV. The data are shown as black points and the total fit function by a blue line. The contributions from the signal, and the low-mass, cross-feed and combinatorial backgrounds are indicated by red (dotted), green (full), magenta (dash-dotted) and black (multiple-dot-dashed) lines, respectively. The bottom figures are the normalised residuals (pull) distributions.

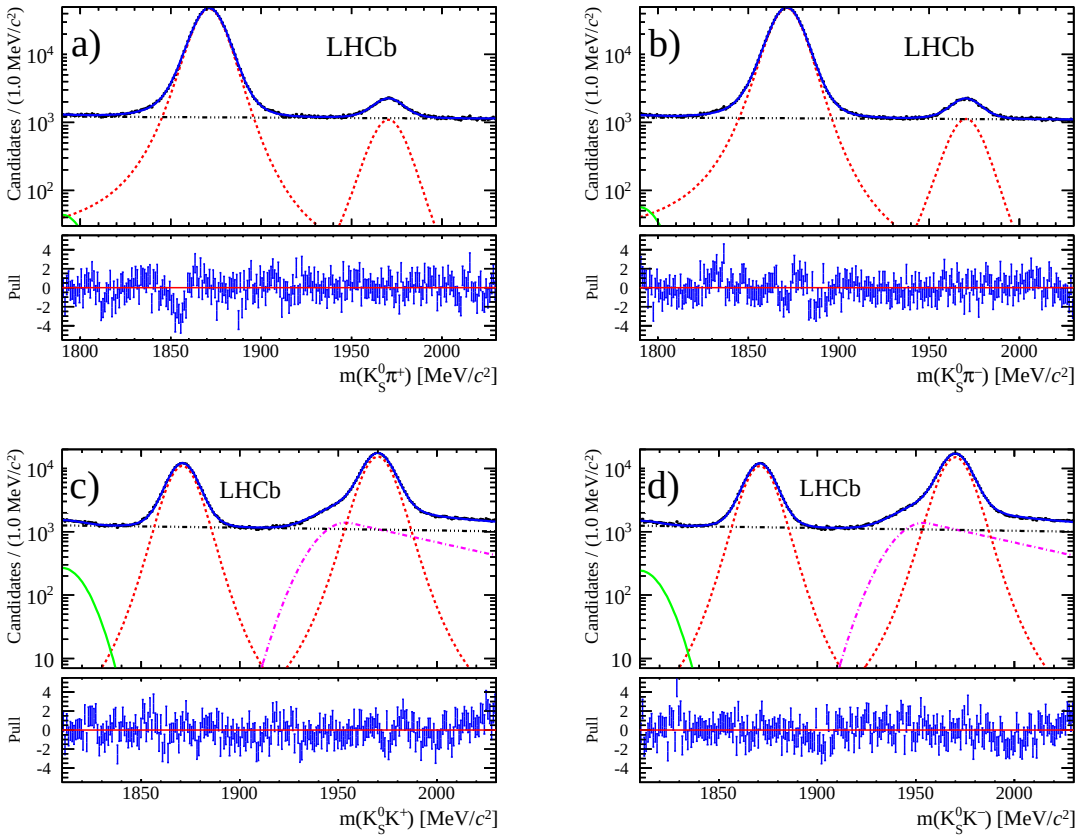

Figure 3: Invariant mass distributions for the a) $D^+_{(s)} \to K^0_S\pi^+$, b) $D^-_{(s)} \to K^0_S\pi^-$, c) $D^+_{(s)} \to K^0_S K^+$ and d) $D^-_{(s)} \to K^0_S K^-$ decay candidates for data taken in the magnetic polarity *Down* configuration at $\sqrt{s} = 8$ TeV. The data are shown as black points and the total fit function by a blue line. The contributions from the signal, and the low-mass, cross-feed and combinatorial backgrounds are indicated by red (dotted), green (full), magenta (dash-dotted) and black (multiple-dot-dashed) lines, respectively. The bottom figures are the normalised residuals (pull) distributions.

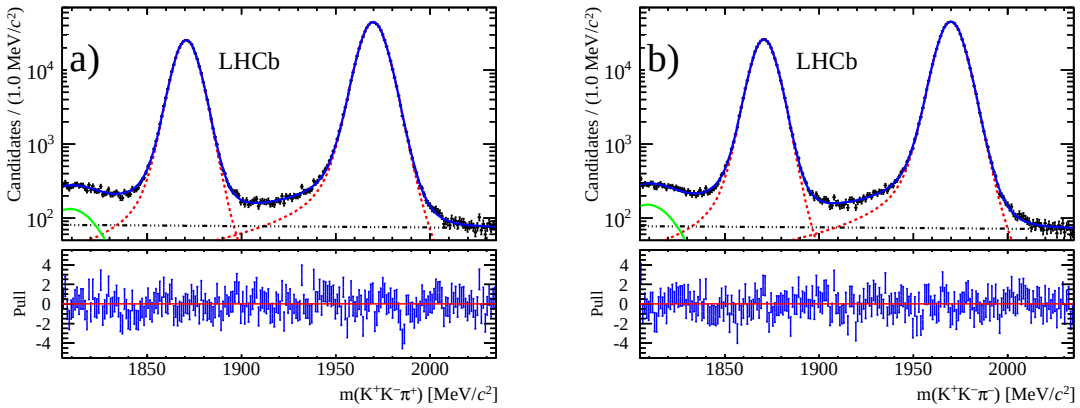

Figure 4: Invariant mass distributions for the a) $D^+_{(s)} \to \phi\pi^+$ and b) $D^-_{(s)} \to \phi\pi^-$ decay candidates for data taken in the magnet polarity *Up* configuration at $\sqrt{s} = 7$ TeV. The data are shown as black points and the total fit function by a blue line. The contributions from the signal, and the low-mass and combinatorial backgrounds are indicated by red (dotted), green (full) and black (multiple-dot-dashed) lines, respectively. The bottom figures are the normalised residuals (pull) distributions.

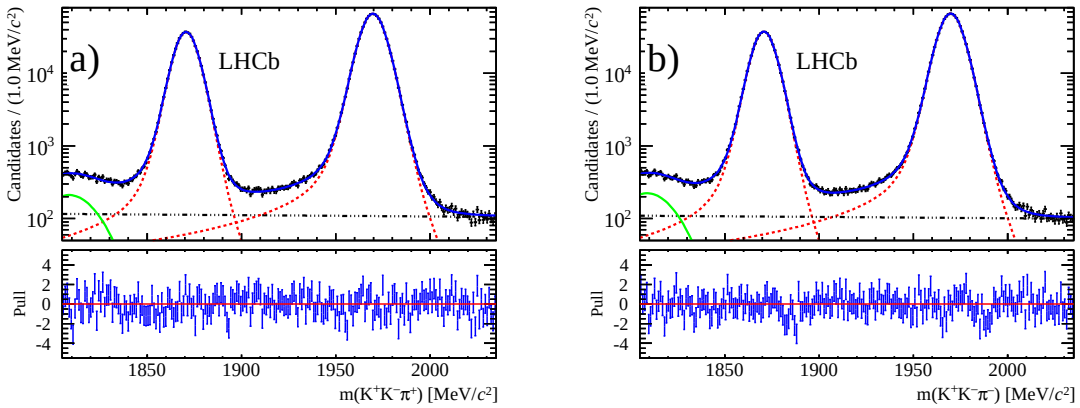

Figure 5: Invariant mass distributions for the a) $D^+_{(s)} \to \phi\pi^+$ and b) $D^-_{(s)} \to \phi\pi^-$ decay candidates for data taken in the magnet polarity *Down* configuration at $\sqrt{s} = 7$ TeV. The data are shown as black points and the total fit function by a blue line. The contributions from the signal, and the low-mass and combinatorial backgrounds are indicated by red (dotted), green (full) and black (multiple-dot-dashed) lines, respectively. The bottom figures are the normalised residuals (pull) distributions.

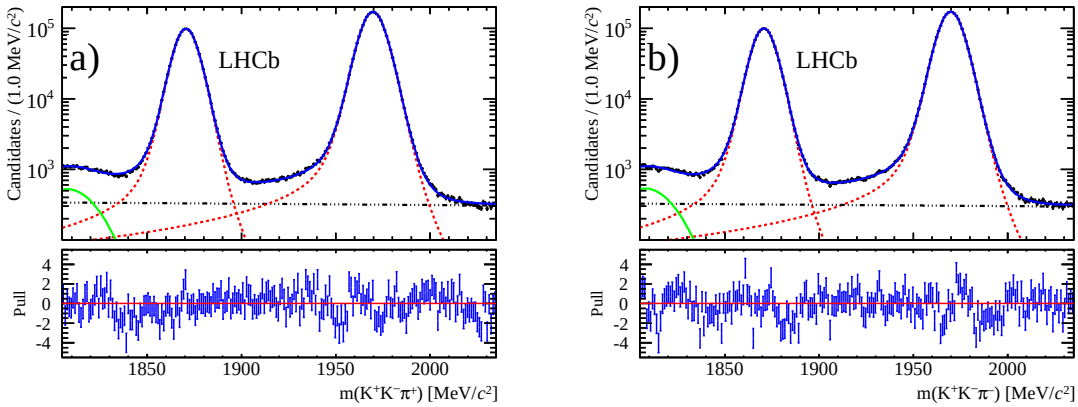

Figure 6: Invariant mass distributions for the a) $D^+_{(s)} \to \phi\pi^+$ and b) $D^-_{(s)} \to \phi\pi^-$ decay candidates for data taken in the magnet polarity *Down* configuration at $\sqrt{s} = 8$ TeV. The data are shown as black points and the total fit function by a blue line. The contributions from the signal, and the low-mass and combinatorial backgrounds are indicated by red (dotted), green (full) and black (multiple-dot-dashed) lines, respectively. The bottom figures are the normalised residuals (pull) distributions.